EPJ Web of Conferences **152**, 07001 (2017) DOI: 10.1051/epjconf/201715207001
Wide-Field Variability Surveys: A 21st Century Perspective

Pulsating stars and the distance scale

Lucas Macri[1,⋆]

[1] *Mitchell Institute for Fundamental Physics & Astronomy and Department of Physics & Astronomy, Texas A&M University, College Station, Texas, United States of America*

Abstract. I present an overview of the latest results from the SH0ES project, which obtained homogeneous *Hubble Space Telescope* (*HST*) photometry in the optical and near-infrared for $\sim$ 3500 and $\sim$ 2300 Cepheids, respectively, across 19 supernova hosts and 4 calibrators to determine the value of H_0 with a total uncertainty of 2.4%.
I discuss the current 3.4σ "tension" between this local measurement and predictions of H_0 based on observations of the CMB and the assumption of "standard" ΛCDM. I review ongoing efforts to reach $\sigma(H_0) = 1\%$, including recent advances on the absolute calibration of Milky Way Cepheid period-luminosity relations (PLRs) using a novel astrometric technique with *HST*.
Lastly, I highlight recent results from another collaboration on the development of new statistical techniques to detect, classify and phase extragalactic Miras using noisy and sparsely-sampled observations. I present preliminary Mira PLRs at various wavelengths based on the application of these techniques to a survey of M33.

1 Introduction & motivation

Pulsating stars have played a key role in the extragalactic distance scale since the discovery of the Cepheid period-luminosity relation (hereafter, PLR, [1]) and its first use ([2]) to calibrate a secondary distance indicator and estimate the local expansion rate of the Universe (hereafter, H_0). Figure 1 shows a schematic representation of the modern extragalactic distance "ladder" based on Cepheids and type Ia supernovae (hereafter, SNe Ia). The latter are excellent "standardizable candles" as first shown by [3]. Further refinements to the calibration of SNe Ia magnitudes based on their light curve properties ([4, 5]) enabled the discovery of dark energy ([6, 7]).

In the two decades since the discovery of dark energy, a considerable amount of theoretical and observational effort has been devoted to understanding its properties. Given an equation of state of dark energy $w = p/\rho$ that evolves with scale factor a as $w = w_0 + w_a(1 - a)$ ([11]), one possible "figure of merit" for dark energy surveys ([9]) is the inverse of the area of the ellipse that represents the allowed parameter space for w_0 and w_a (see left panel of Fig. 2). The combination of SNe Ia with other observational probes of dark energy (such as baryon acoustic oscillations and the cosmic microwave background) can significantly improve this figure of merit by reducing the impact of degeneracies affecting any given method. More precise and accurate determinations of H_0 play a critical role in this effort, and their impact can be quite significant if $\sigma(H_0) \lesssim 2\%$ ([10]; see right panel of Fig. 2).

⋆ lmacri@tamu.edu

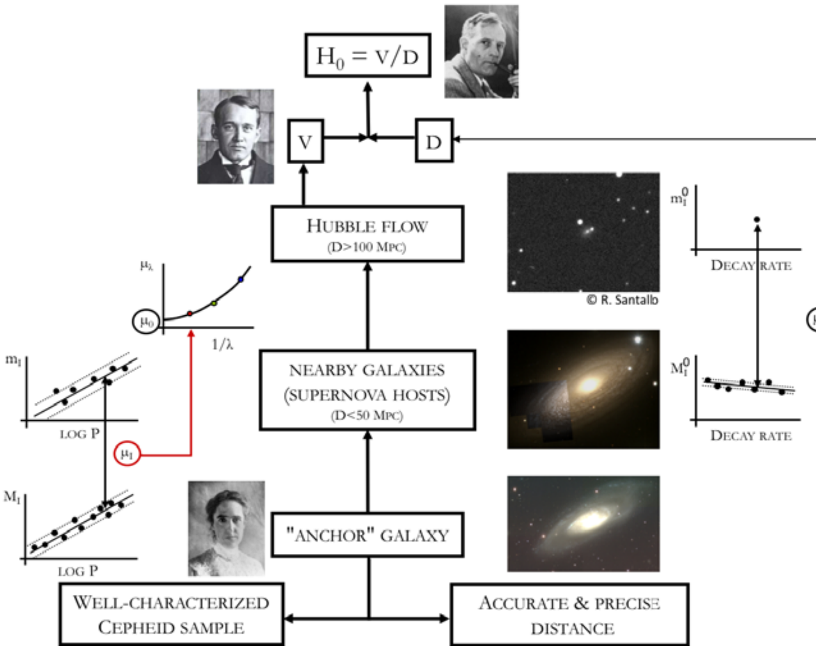

Figure 1. Steps to the Hubble Constant. This distance ladder begins with the absolute calibration of the Cepheid PLR in one or more nearby "anchor" galaxies that have well-characterized samples of these variables as well as precise and accurate distances. The second "rung" in the ladder consists of multi-wavelength observations of Cepheid-bearing galaxies that have hosted modern and "ideal" SNe Ia (low reddening, well-sampled digital light curve). This enables a robust calibration of the SN Ia luminosity-decline rate relation (or a more sophisticated formulation of this secondary distance indicator). The last "rung" uses SNe Ia in the Hubble flow. Pictured are H. Leavitt (discoverer of the Cepheid PLR), V. Slipher (pioneer of galaxy redshifts) and E. Hubble.

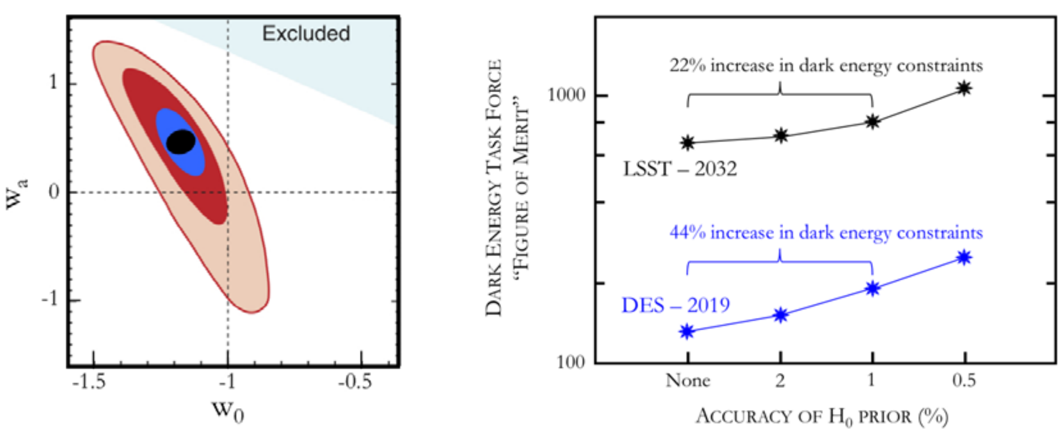

Figure 2. Left: Current and anticipated constraints on the equation of state of dark energy. Red/salmon contours represent $1/2\sigma$ constraints from [8]; blue and black denote expected 2σ constraints by DES and LSST, respectively. Right: Improvement on the Dark Energy Task Force figure of merit ([9]) as a function of $\sigma(\mathrm{H}_0)$ ([10]).

2 SH0ES: A decade of efforts leading to $\sigma(\mathrm{H_0}) = 2.4\%$

Motivated by the above, the SH0ES team (PI: A. Riess) has worked over the past decade to measure $\mathrm{H_0}$ with increasing accuracy and precision. Our first two publications ([12, 13]) represented improvements of 2× and 3× ($\sigma(\mathrm{H_0}) = 4.8\%, 3.3\%$) over previous efforts ([14, 15]), while our most recent work ([16, 17]) halves our initial uncertainty ($\sigma(\mathrm{H_0}) = 2.4\%$). Figure 3 shows the Cepheid-bearing galaxies used in our latest analysis, while Figure 4 shows the corresponding I and H PLRs with $\sim$ 3500 and $\sim$ 2300 variables, respectively.

Figure 5 shows the evolution of the SH0ES error budget over time. Our initial improvement ([12]) over previous work was the result of building a differential distance ladder based exclusively on *HST* photometry of Cepheids (negating systematic uncertainties due to the mix of ground- and space-based measurements) and focused on near-infrared observations (minimizing systematic uncertainties due to extinction and metallicity). Our second publication ([13]) benefited from a substantial increase in the number of near-infrared Cepheid observations, made possible by the installation of WFC3 on *Hubble*. Our third and latest determination ([16]) is based on a significantly larger number of supernova host galaxies, which were more efficiently surveyed for Cepheids by using a long-pass filter ([17]). Equally critical along the way have been the improvements on the distance estimates for our "anchor" galaxies, which are based on independent techniques: maser observations for NGC 4258 ([18, 19]); detached eclipsing binaries for the LMC ([20]); and parallaxes for Milky Way Cepheids ([21–24]).

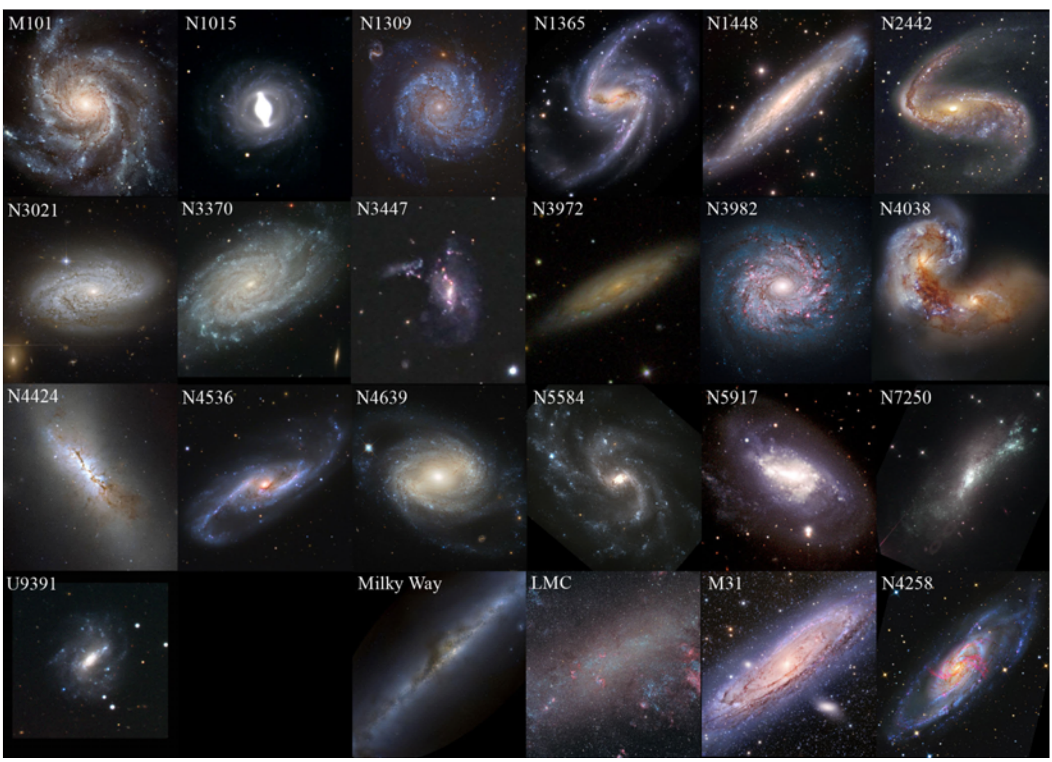

Figure 3. Cepheid-bearing galaxies used in the most recent determination of $\mathrm{H_0}$ by the SH0ES team ([16]). Based on [17].

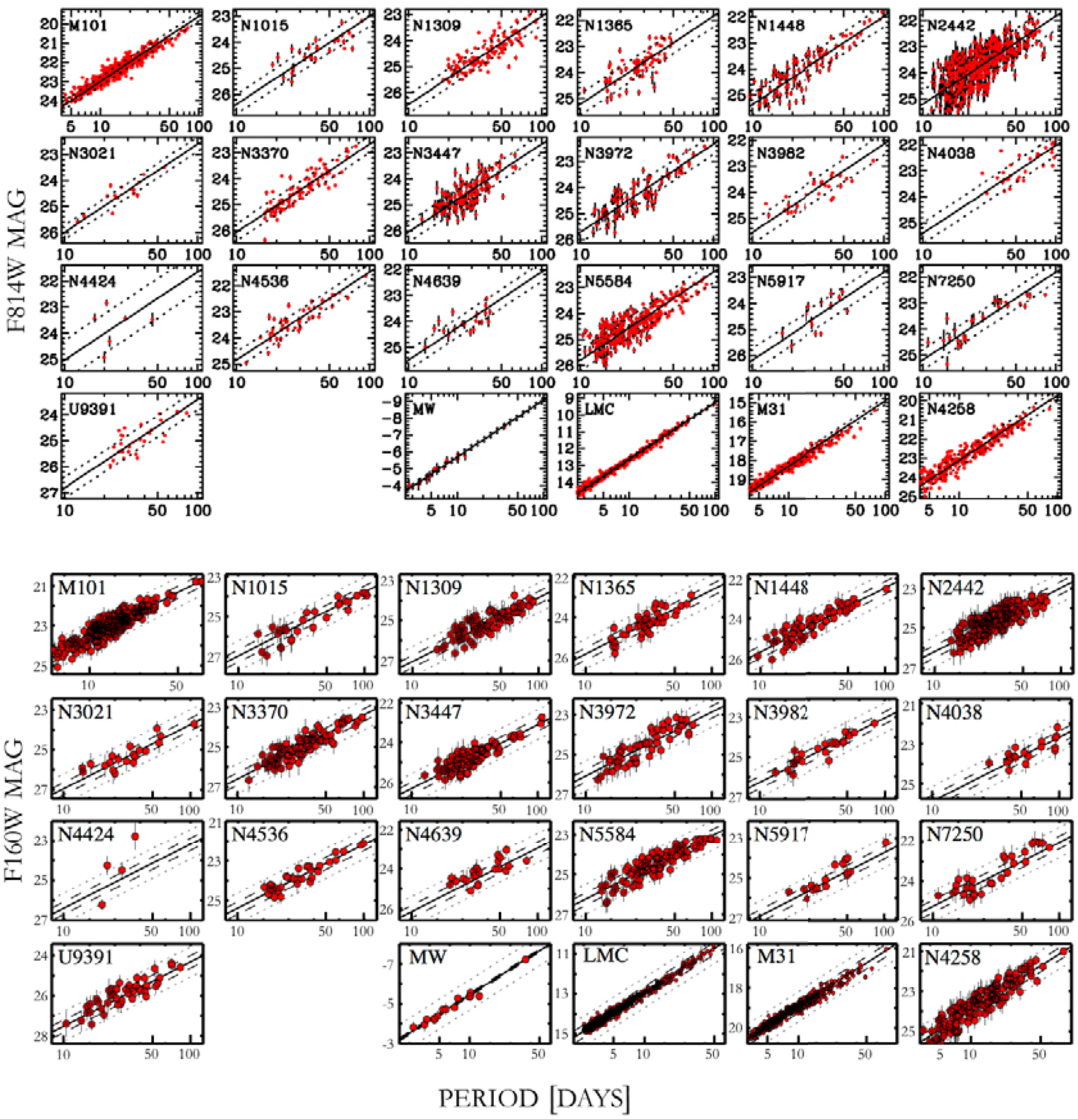

Figure 4. Cepheid period-luminosity relations in *F814W* (top) and *F160W* (bottom) for all galaxies in the most recent study by the SH0ES team. Based on [16, 17].

3 Current and future steps towards $\sigma(\mathrm{H}_0) = 1\%$

The current measurement of H_0 by the SH0ES team ([16]) is larger by $\sim 3.4\sigma$ than the *predicted* value by [25]. The latter is inferred using the Baryon Acoustic Oscillation method, calibrated from observations of the Cosmic Microwave Background and assuming a specific cosmological model (standard ΛCDM). While the discrepancy may be due to systematic effects on one or both sides, an intriguing possibility is that the difference might be due to an additional component in the cosmological model

DOI: 10.1051/epjconf/201715207001

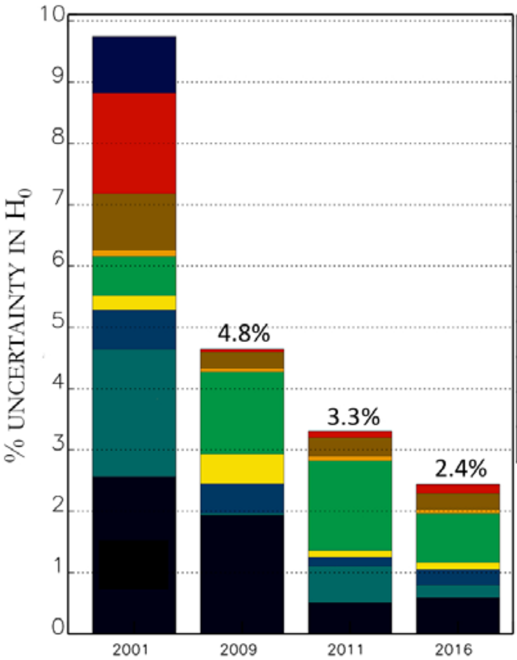

TERM	KP	'09	'11	'16
	%			
ABSOLUTE SCALE	5.0	3.0	1.3	1.3
REDDENING & ZEROPOINTS (ANCHOR-TO-HOSTS)	4.5	0.3	1.4	0.7
P-L SLOPE, D LOG P (ANCHOR-TO-HOSTS)	4.0	0.5	0.6	0.5
METALLICITY DEPENDENCE (ANCHOR-TO-HOSTS)	3.0	1.1	1.0	0.8
GROUND/HST CROSS-CALIBRATION	3.0	--	--	--
MEAN OF SN IA CALIBRATORS	2.5	2.5	1.9	1.3
MEAN OF P-L IN ANCHOR(S)	2.5	1.5	0.8	0.7
MEAN OF P-L IN SN HOSTS	1.5	1.5	0.6	0.4
SN IA M-Z RELATION	1.0	0.5	0.4	0.4
ANALYSIS SYSTEMATICS	??	1.3	1.0	0.9
TOTAL	10	4.8	3.3	2.4

Figure 5. Evolution of the error budget for H_0 in various iterations of the SH0ES project ([12, 13, 16]), compared with the *HST* Key Project on the Distance Scale ([14]). Based on [16].

([26]). Figure 6, adapted from [27], shows that most of the "tension" can be alleviated by including an extra relativistic species in the early Universe.

Given this intriguing discrepancy, further work is warranted to reach $\sigma(H_0) = 1\%$. This will require a better absolute calibration of the Cepheid PLR and a significant increase in the number of SNe Ia hosts with Cepheid distances. Regarding the first issue, the SH0ES team has used a novel observing technique available with WFC3 ("spatial scanning") to measure parallaxes to 19 Milky Way Cepheids located at considerable greater distances ($D \lesssim 4$ kpc) than the previously-studied 10 variables ($D \lesssim 500$ pc). Beyond the significant increase in sample size, our targets span a range in periods that is better matched to the extragalactic sample and helps to minimize any remaining systematics associated with variations in the slope of the PLR (see Fig. 7). The two parallaxes published thus far by this program ([23, 24]) are also significantly more precise than previous determinations despite the considerably smaller parallax signal.

The *Gaia* mission is expected to discover and measure high-quality parallaxes for thousands of Cepheids in the Milky Way ([28]), and to provide much-improved distances for the currently-known variables of this type. This should yield a sub-percent calibration of the Galactic PLR, and it will be critical to place as many of these variables as possible on the same photometric system used to study extragalactic targets to avoid further systematic uncertainties. To this end, the SH0ES team has already obtained *HST* photometry for 50 Cepheids that are expected to have the highest-quality parallaxes from *Gaia*.

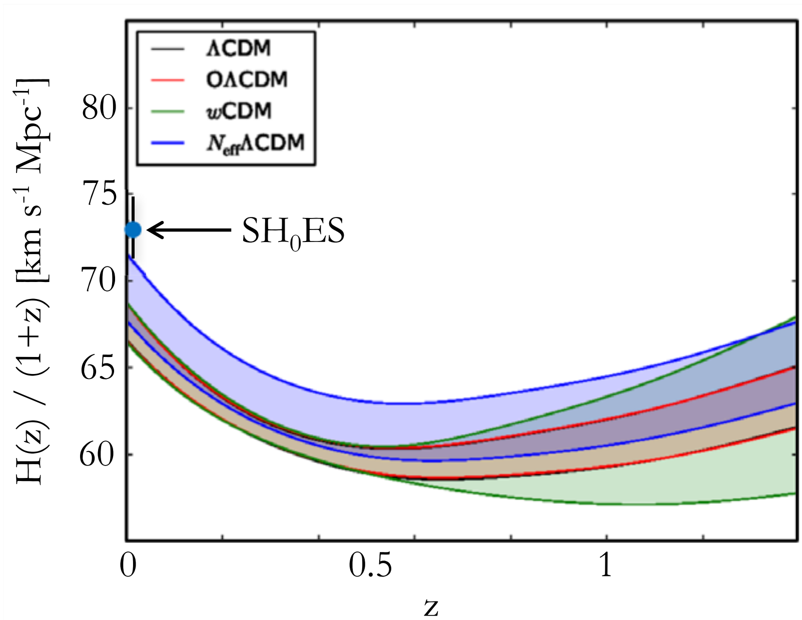

Figure 6. Comparison of *predicted* values of H(z) for different cosmological models vs. H_0 measured by SH0ES ([16]). Based on [27].

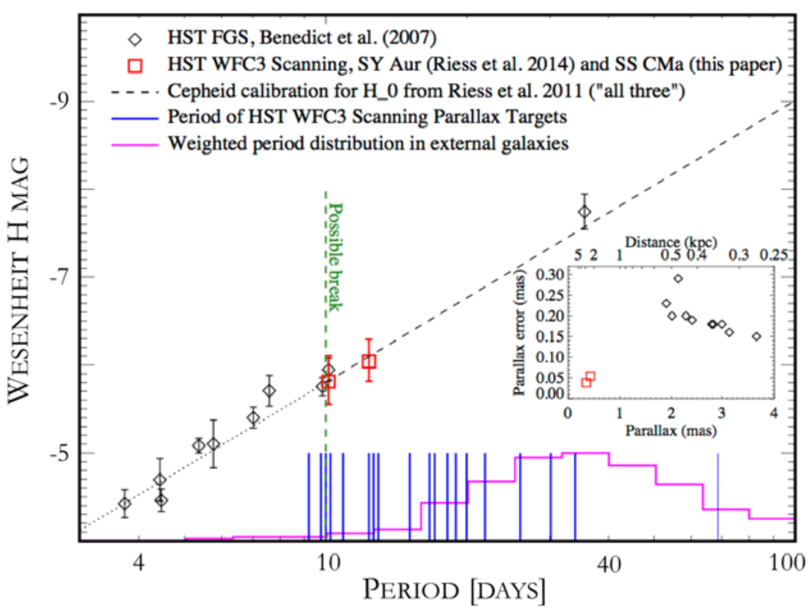

Figure 7. Improved Galactic Cepheid PLR using parallaxes measured with novel *HST* technique, and prospects for future improvement. Based on [24].

DOI: 10.1051/epjconf/201715207001

4 Miras: new techniques and prospects for LSST

Mira variables could play a significant role in the extragalactic distance scale during the next decade, as part of the quest to reach $\sigma(H_0) = 1\%$ with facilities such as *JWST* and *WFIRST*. Given their intermediate-mass progenitors, they are more plentiful than Cepheids and are present in early-type galaxies. As shown in Figure 8, oxygen-rich Miras rival the luminosities of Cepheids at K and exhibit a tight PLR at near-infrared wavelengths ([29, 30]). Besides their significantly longer periods relative to Cepheids, another possible roadblock to their wide use is the large variations exhibited by their light curves from cycle to cycle. This complicates the determination of periods using traditional techniques ([31, 32]) on sparsely-sampled light curves.

A collaboration between statisticians and astronomers at Texas A&M University has recently yielded new techniques for determining the periods of Miras in the regime of sparsely-sampled, noisy light curves ([36]). We used the OGLE-III light curves of Miras in the LMC and downsampled them to simulate time-series observations with more typical coverage and photometric precision for extragalactic variables. We developed a novel periodogram based on the Gaussian Process method and tested it using the simulated light curves. We found the new algorithm outperformed the traditional period-finding techniques and was able to successfully recover periods for ~ 70% of the variables (see Fig. 9). We applied the technique to I-band observations of M33 ([37, 38]) and discovered over 1800 Mira candidates in this galaxy ([35]). We matched our optical catalog with NIR and MIR observations from [39, 40] and obtained PLRs that compare favorably to their LMC counterparts (see Fig. 10).

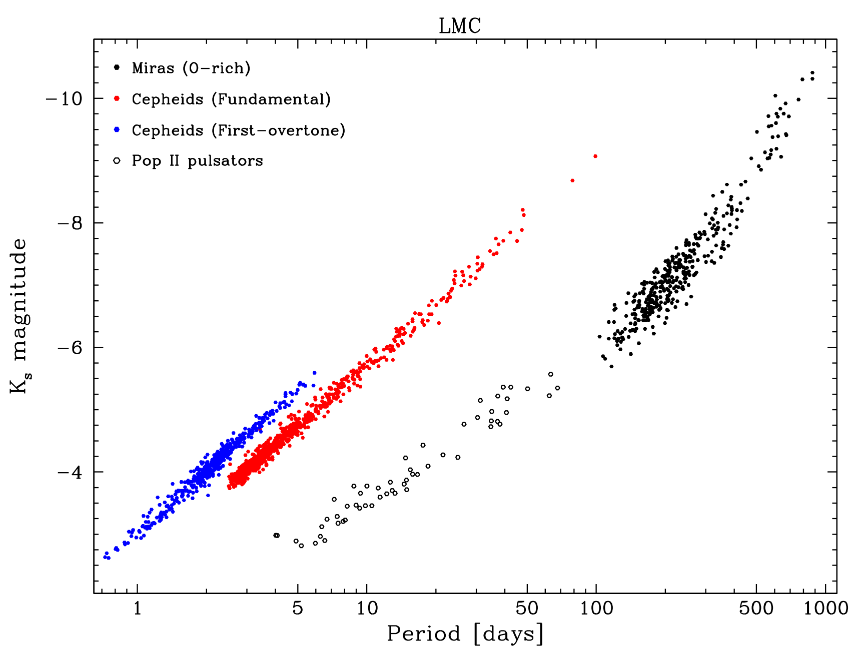

Figure 8. Comparison of K-band PLRs for various types of pulsating stars. Based on [33], [34] and [35] for Cepheids, Pop. II pulsators and O-rich Miras, respectively.

 DOI: 10.1051/epjconf/201715207001

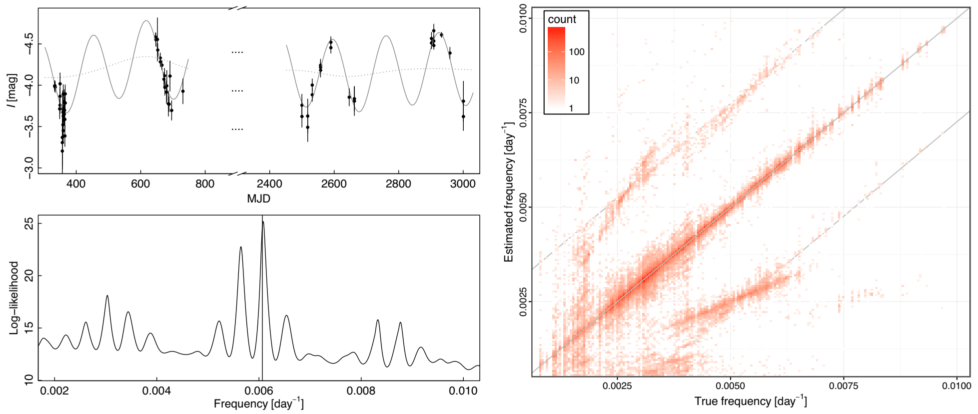

Figure 9. Application of the Gaussian Process to model simulated Mira light curves that are noisy and sparsely sampled (left) and success in recovering the known periods of the variables used to generate the simulations (right). Based on [36].

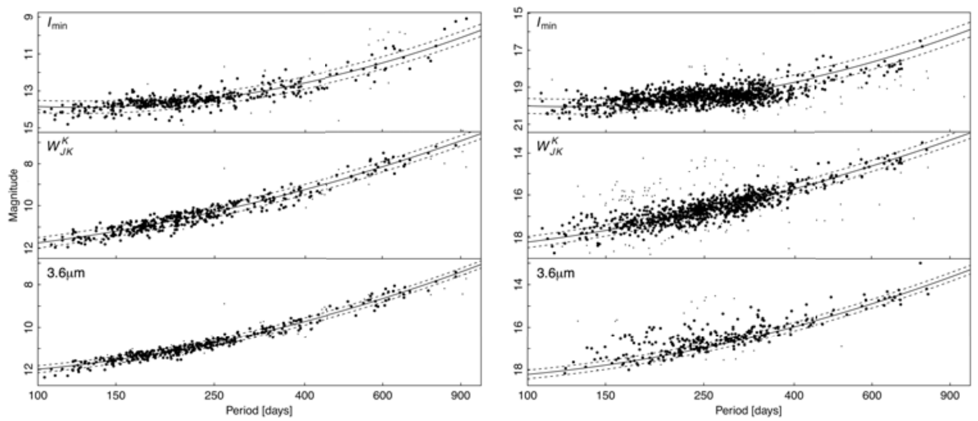

Figure 10. Mira PLRs in various bands for O-rich variables in the LMC (left) and M33 (right). Based on [35].

Motivated by the success of the Gaussian Process periodogram at detecting Mira candidates in M33, we carried out additional simulations to investigate the usefulness of the expected LSST cadence for the "deep-wide-fast" survey for finding O-rich variables in galaxies with $D \lesssim 15$ Mpc ([41]). The preliminary results, shown in Figure 11, are quite encouraging. The largest yield is expected in NGC 5128, given its relatively close distance and large mass; ~ 29000 O-rich Miras could be detected. We expect that LSST will be able to detect 100 or more Miras in ~ 70 galaxies, for a final yield of $\sim 2 \times 10^5$ variables by the end of its initial decade-long survey. Most detections will occur in i, and $> 75\%$ of the variables should have $i - z$ colors. Follow-up of selected subsets of these variables with *JWST*, *WFIRST* or other space-based NIR missions would yield accurate and precise distances to the host galaxies.

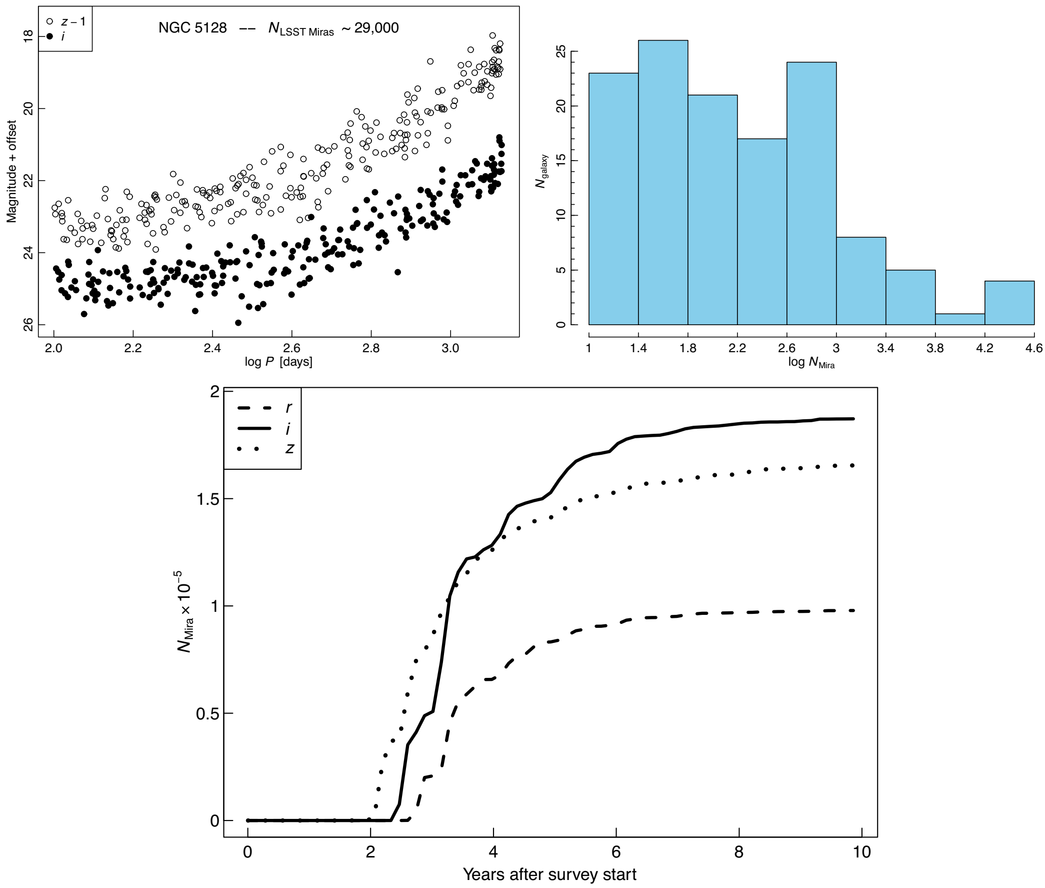

Figure 11. Prospects for detection of O-rich Miras with LSST. Upper left: simulated PLR for Miras in NGC 5128 (only a subset of the ∼ 29000 expected variables are plotted). Upper right: Number of galaxies in which LSST should detect a given number of Miras. Bottom: Detectability of Miras with LSST as a function of time since the start of the survey. Based on [41].

Acknowledgments: *HST* observations of extragalactic Cepheids were supported by NASA/STScI through HST-GO awards 9810, 10399, 10802, 11570, 12880 and 13647. *HST* studies of Milky Way Cepheids were supported by NASA/STScI through HST-GO awards 12679, 12879, 13334, 13335, 13344, 13678, 13686, 13928, 14062 and 14648. The ground-based observations of Cepheids and Miras were supported by the US National Science Foundation through grant AST-1211603. All projects received additional support from the Mitchell Institute for Fundamental Physics & Astronomy at Texas A&M University.

References

[1] H.S. Leavitt, E.C. Pickering, Harvard College Observatory Circular **173**, 1 (1912)
[2] E. Hubble, PNAS **15**, 168 (1929)
[3] M.M. Phillips, ApJL **413**, L105 (1993)

[4] M. Hamuy, M.M. Phillips, N.B. Suntzeff, R.A. Schommer, J. Maza, R. Aviles, AJ **112**, 2391 (1996)
[5] A.G. Riess, W.H. Press, R.P. Kirshner, ApJ **473**, 88 (1996)
[6] A.G. Riess, A.V. Filippenko, P. Challis, A. Clocchiatti, A. Diercks, P.M. Garnavich, R.L. Gilliland, C.J. Hogan, S. Jha, R.P. Kirshner et al., AJ **116**, 1009 (1998)
[7] S. Perlmutter, G. Aldering, G. Goldhaber, R.A. Knop, P. Nugent, P.G. Castro, S. Deustua, S. Fabbro, A. Goobar, D.E. Groom et al., ApJ **517**, 565 (1999)
[8] G. Hinshaw, D. Larson, E. Komatsu, D.N. Spergel, C.L. Bennett, J. Dunkley, M.R. Nolta, M. Halpern, R.S. Hill, N. Odegard et al., ApJS **208**, 19 (2013)
[9] A. Albrecht, G. Bernstein, R. Cahn, W.L. Freedman, J. Hewitt, W. Hu, J. Huth, M. Kamionkowski, E.W. Kolb, L. Knox et al., arXiv (2006), `astro-ph/0609591`
[10] D.H. Weinberg, M.J. Mortonson, D.J. Eisenstein, C. Hirata, A.G. Riess, E. Rozo, Phys. Rep. **530**, 87 (2013)
[11] E.V. Linder, PRL **90**, 091301 (2003)
[12] A.G. Riess, L. Macri, S. Casertano, M. Sosey, H. Lampeitl, H.C. Ferguson, A.V. Filippenko, S.W. Jha, W. Li, R. Chornock et al., ApJ **699**, 539 (2009)
[13] A.G. Riess, L. Macri, S. Casertano, H. Lampeitl, H.C. Ferguson, A.V. Filippenko, S.W. Jha, W. Li, R. Chornock, ApJ **730**, 119 (2011)
[14] W.L. Freedman, B.F. Madore, B.K. Gibson, L. Ferrarese, D.D. Kelson, S. Sakai, J.R. Mould, R.C. Kennicutt, Jr., H.C. Ford, J.A. Graham et al., ApJ **553**, 47 (2001)
[15] A. Sandage, G.A. Tammann, A. Saha, B. Reindl, F.D. Macchetto, N. Panagia, ApJ **653**, 843 (2006)
[16] A.G. Riess, L.M. Macri, S.L. Hoffmann, D. Scolnic, S. Casertano, A.V. Filippenko, B.E. Tucker, M.J. Reid, D.O. Jones, J.M. Silverman et al., ApJ **826**, 56 (2016)
[17] S.L. Hoffmann, L.M. Macri, A.G. Riess, W. Yuan, S. Casertano, R.J. Foley, A.V. Filippenko, B.E. Tucker, R. Chornock, J.M. Silverman et al., ApJ **830**, 10 (2016)
[18] J.R. Herrnstein, J.M. Moran, L.J. Greenhill, P.J. Diamond, M. Inoue, N. Nakai, M. Miyoshi, C. Henkel, A. Riess, Nature **400**, 539 (1999)
[19] E.M.L. Humphreys, M.J. Reid, J.M. Moran, L.J. Greenhill, A.L. Argon, ApJ **775**, 13 (2013)
[20] G. Pietrzyński, D. Graczyk, I.B. Gieren, W. Thompson, B. Pilecki, A. Udalski, S. Soszyński, I. Kozłowski, P. Konorski, G. Suchomska, K. Bono, P.G.P. Moroni, S. Villanova et al., Nature **495**, 76 (2013)
[21] G.F. Benedict, B.E. McArthur, M.W. Feast, T.G. Barnes, T.E. Harrison, R.J. Patterson, J.W. Menzies, J.L. Bean, W.L. Freedman, AJ **133**, 1810 (2007)
[22] F. van Leeuwen, A&A **474**, 653 (2007)
[23] A.G. Riess, S. Casertano, J. Anderson, J. MacKenty, A.V. Filippenko, ApJ **785**, 161 (2014)
[24] S. Casertano, A.G. Riess, J. Anderson, R.I. Anderson, J.B. Bowers, K.I. Clubb, A.R. Cukierman, A.V. Filippenko, M.L. Graham, J.W. MacKenty et al., ApJ **825**, 11 (2016)
[25] Planck Collaboration, et al., A&A **596**, A107 (2016)
[26] C. Dvorkin, M. Wyman, D.H. Rudd, W. Hu, Phys Rev D **90**, 083503 (2014)
[27] A.J. Cuesta, L. Verde, A. Riess, R. Jimenez, MNRAS **448**, 3463 (2015)
[28] F. Windmark, L. Lindegren, D. Hobbs, A&A **530**, A76 (2011)
[29] I.S. Glass, T. Lloyd Evans, Nature **291**, 303 (1981)
[30] P.A. Whitelock, M.W. Feast, F. van Leeuwen, MNRAS **386**, 313 (2008)
[31] N.R. Lomb, Ap&SS **39**, 447 (1976)

[32] J.D. Scargle, ApJ **263**, 835 (1982)
[33] L.M. Macri, C.C. Ngeow, S.M. Kanbur, S. Mahzooni, M.T. Smitka, AJ **149**, 117 (2015)
[34] A. Bhardwaj, L.M. Macri, M. Rejkuba, S.M. Kanbur, C.C. Ngeow, H.P. Singh, AJ **153**, 154 (2017)
[35] W. Yuan, S. He, L.M. Macri, J. Long, J.Z. Huang, AJ **153**, 170 (2017)
[36] S. He, W. Yuan, J.Z. Huang, J. Long, L.M. Macri, AJ **152**, 164 (2016)
[37] L.M. Macri, K.Z. Stanek, D.D. Sasselov, M. Krockenberger, J. Kaluzny, AJ **121**, 861 (2001)
[38] A. Pellerin, L.M. Macri, ApJS **193**, 26 (2011)
[39] A. Javadi, M. Saberi, J.T. van Loon, H. Khosroshahi, N. Golabatooni, M.T. Mirtorabi, MNRAS **447**, 3973 (2015)
[40] T.A. Thompson, J.L. Prieto, K.Z. Stanek, M.D. Kistler, J.F. Beacom, C.S. Kochanek, ApJ **705**, 1364 (2009)
[41] W. Yuan, Ph.D. thesis, Texas A&M University (2017)